Monolithic Integrated Millimeter-Wave IMPATT Transmitter in Standard CMOS Technology

Talal Al-Attar and Thomas H. Lee, *Member, IEEE*

***Abstract*—This paper describes impact avalanche transit time (IMPATT) diodes fabricated in 0.18-μm standard complementary metal–oxide–semiconductor technology to enable operation at 77 GHz. The lateral IMPATT diodes are integrated with a microstrip patch antenna, modified to provide impedance matching and widen the tuning range. The antenna dimensions and the impedance matching are designed using the high-frequency electromagnetic field solver Sonnet. The output spectrum has no visible spurious components. The transmitted power is −62 dBm at 76 GHz. The measured frequency is within 1.3% of the simulated value. It is hoped that this device will find application in automotive and communication systems.**

***Index Terms*—Complementary metal–oxide–semiconductor technology (CMOS), impact avalanche transit time (IMPATT) diode, microstrip patch antenna, Sonnet, stub, vector network analyzer (VNA).**

I. Introduction

IMPACT avalanche transit time (IMPATT) diodes are well known for their performance at frequencies extending into the millimeter-wave range. Many radar systems have a need for high power microwave sources in their transmitters that can only be addressed by the use of IMPATT diodes [1]. Their small size and light weight are advantageous in these systems when compared with alternatives. So far, monolithic millimeter-wave IMPATT oscillators have been fabricated in GaAs [2], InP [3], Si [4], and SiGe [1] processes. Most IMPATT diodes are produced in discrete form and operated in external circuits, limiting their widespread use in compact, lightweight, and low-cost systems that require higher degrees of integration. Recently, monolithic integration of lateral IMPATT diodes [5] with a microstrip patch antenna at 77 GHz has been achieved in standard complementary metal–oxide–semiconductor (CMOS) technology [6]. This CMOS transmitter is particularly appealing from a cost reduction and system integration standpoint. In this work, the antenna is designed as a radiator and a resonator at the same time to minimize the required chip area. In addition, a study of the effect of different feed type and feed locations to match the IMPATT impedance is presented. Such a topology reduces parasitic losses, since no microstrip line is necessary to connect the oscillator to the antenna. At the same time, matching the IMPATT to the antenna is facilitated by integrating three diodes and three stubs along one of the radiating edges.

In this study, the antenna impedance seen by the IMPATT diode was estimated by the electromagnetic (EM) field solver Sonnet, while the impedance of the IMPATT diode was characterized by on-wafer measurements in a standard CMOS process [5]. In Section II, we describe the design of the 77-GHz transmitter, followed by experimental results of the system in Section III.

Manuscript received April 5, 2005; revised July 19, 2005.

The authors are with the Center for Integrated Systems, Stanford University, Stanford, CA 94305-4070 USA.

Digital Object Identifier 10.1109/TMTT.2005.858379

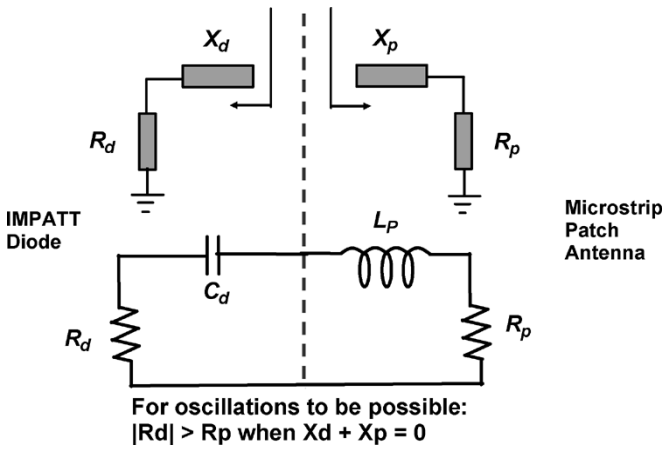

Fig. 1. Oscillator block diagram.

II. Oscillator Design

A necessary condition for steady-state oscillation is a zero sum for the circuit and device impedances at the steady-state operating point (Fig. 1).

The microwave negative resistance of an IMPATT diode arises out of a phase difference between the RF voltage and RF current [7]. This phase difference is produced by the lagging RF current generated in the space charge layer with respect to the applied RF voltage.

The time delay inherent in the buildup of the avalanche current is augmented by the transit delay experienced by the charge carriers in crossing the drift region at saturated drift velocity. In order for the diode to operate as a stable oscillator, the negative conductance of the diode must decrease with increasing RF voltage. The RF voltage across the diode will grow until the admittance of the diode is balanced by the admittance of the microwave circuit.

A. Lateral IMPATT Diode

The cross section of the lateral IMPATT diode is shown in Fig. 2. The diode has a single drift region. The p^+, n, and n^+ regions of the IMPATT diode are implemented using standard source/drain, n-well, and ohmic contact diffusion regions, respectively. The impedance of the diode is measured up to

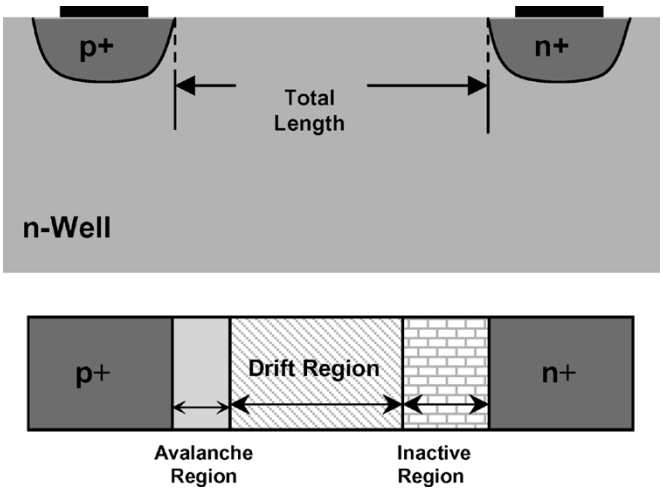

Fig. 2. Lateral IMPATT diode structure, showing the avalanche, drift, and inactive regions.

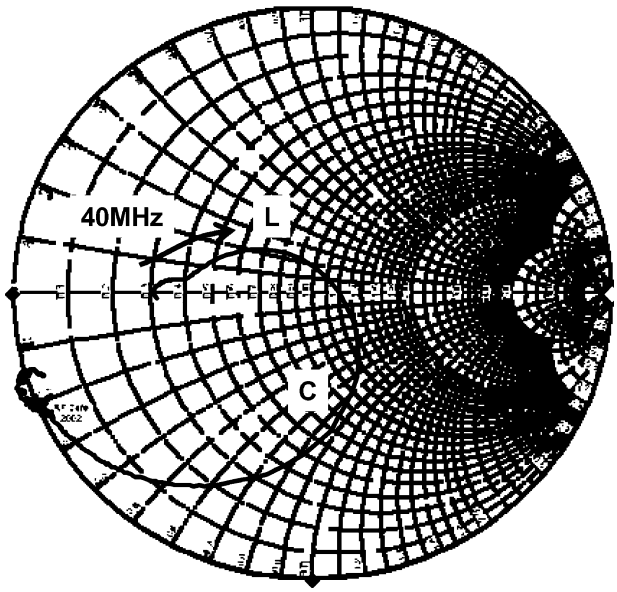

Fig. 3. Measured reflection coefficient of an IMPATT diode at $V_{\rm bias} = 11$ V and $I_{\rm diode} = 30$ mA prior to deembedding.

110 GHz by means of a vector network analyzer (VNA) connected to a CASCADE wafer prober. To minimize the influence of the measurement setup on the diodes, a constant VNA output power of -20 dBm is used. The Smith chart in Fig. 3 provides the reflection coefficient prior to deembedding. At certain frequencies, it becomes greater than 1, as needed to enable oscillation. With open and short structures, the impedance of the parallel and series parasitics (Fig. 4) are estimated to allow deembedded measurements of diode impedance, presented in Fig. 5.

B. Monolithic Resonator/Antenna

The structure of a microstrip patch antenna is particularly amenable to the connection of an active one-port device. One terminal connects to the patch proper, and the other connects to the ground plane. The direct current (dc) bias for the active device is then simply applied between the patch and the ground

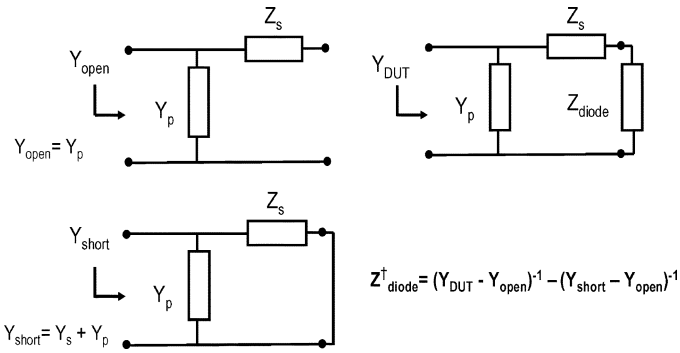

Fig. 4. Equivalent circuit of a coplanar waveguide with parallel and series parasitics.

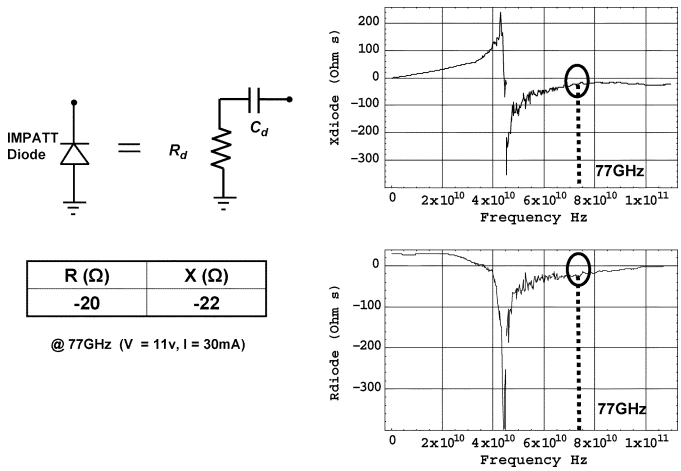

Fig. 5. Measured IMPATT impedance after deembedding at 77 GHz and the IMPATT diode equivalent model.

plane. Simulations reveal that the CMOS IMPATTs are capable of sustaining oscillation at 77 GHz, provided that the resonator resistance is below 20 Ω, and the reactive parts of the antenna and the diode impedances cancel [8].

The impedance seen by the IMPATT diode was calculated using Sonnet. This simulation includes the relevant losses at 77 GHz, such as dielectric, ohmic, radiation, and surface wave losses. The simulation results provide the input impedance, gain, radiation pattern, and radiation efficiency of the antenna.

By examining various candidate layout structures, a 750×1850 μm microstrip patch antenna (Fig. 6) is found to best match the impedance requirements of the IMPATT diode.

The diode's depletion region capacitance introduces a loading effect, so that the length of the patch antenna is reduced relative to that of an equivalent standalone resonator operating at the same frequency. The calculated input impedance of the microstrip patch antenna seen by the IMPATT diode versus frequency is shown in Fig. 7. Since a match is obtained when $Z_{\rm diode} + Z_{\rm antenna} = 0$, the intersection between the negative reactance of the IMPATT diode and the reactance of the microstrip patch antenna determines the oscillation frequency. Supplementing simulations with measurements, the loaded Q is determined to be approximately 7 in this structure.

After selecting the antenna dimensions, we optimized the feedpoint location and the feed type from the IMPATT diode to the antenna as shown in Fig. 8. The tapered feed, with a length

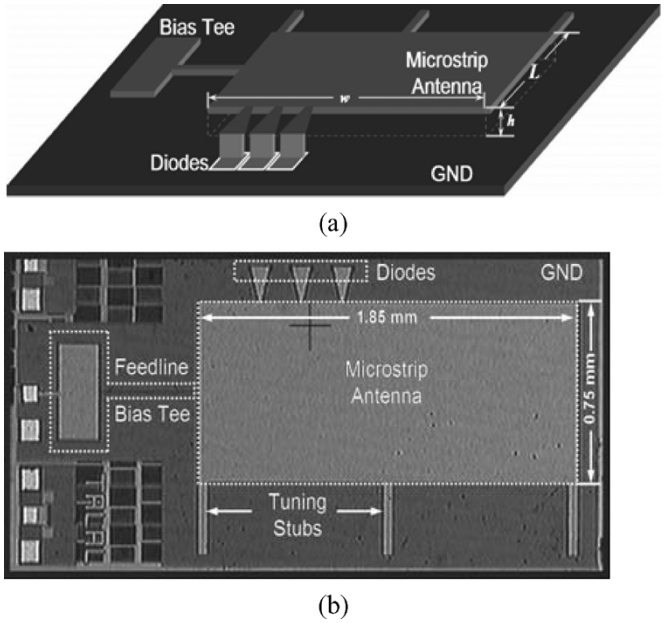

Fig. 6. Monolithic IMPATT transmitter in standard CMOS technology. (a) Layout of the integrated transmitter. (b) Die photograph.

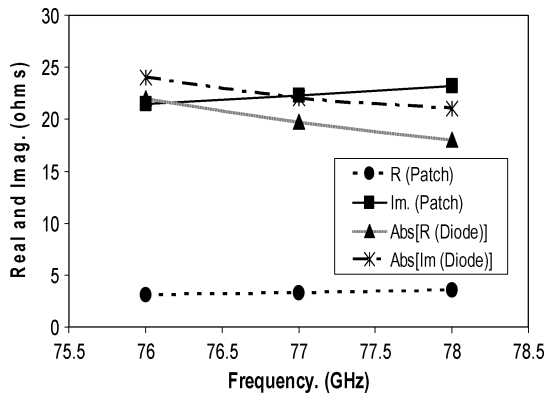

Fig. 7. Real and imaginary parts of the IMPATT diode and microstrip patch antenna impedances.

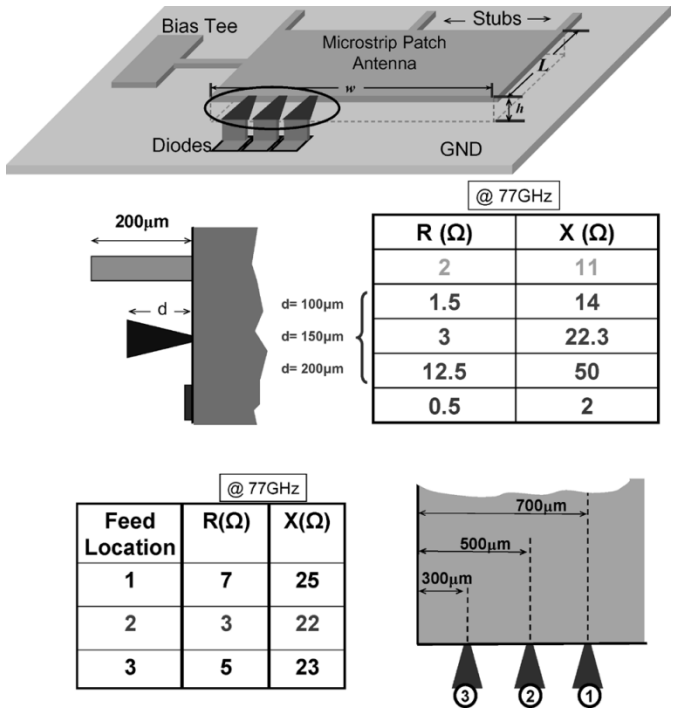

@ 77GHz

R (Ω)	X (Ω)
2	11
1.5	14
3	22.3
12.5	50
0.5	2

@ 77GHz

Feed Location	R(Ω)	X(Ω)
1	7	25
2	3	22
3	5	23

Fig. 8. Feedpoint location and the feed type from the IMPATT diode to the patch antenna.

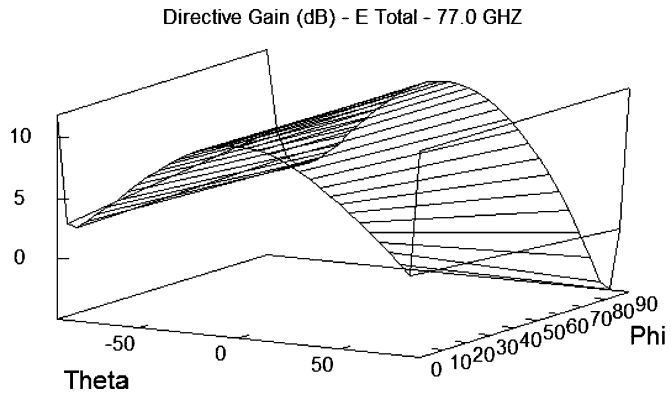

Fig. 9. Simulated directive gain of the CMOS microstrip patch antenna.

of 150 μm, provides the best matching range with respect to the measured IMPATT impedance.

To provide multiple designs, three identical diodes (100×0.45 μm) are placed in the layout, each feeding the antenna at different locations. Diodes can be tested individually by isolating the desired one using a YAG laser. This provides a means of finding the best matching location postfabrication.

Simulations of antenna performance comprehend multiple factors, such as the dielectric cover (passivation layer), finite ground plane, as well as the substrate doping profile of the CMOS technology used. The simulated directive gain of the antenna is 11 dB, as shown in Fig. 9, assuming a 4-μm dielectric thickness. This value of gain implies the necessity of some form of beam shaping for most practical applications. Furthermore, three 50×300 μm stubs are added to the antenna (Fig. 8). The stubs connect to one of the radiating edges of the antenna to provide a means for some postfabrication tuning. Altogether, the real and the imaginary parts of the antenna input impedance can be adjusted over a range of 20% and 3%, respectively.

The parasitics introduced by the vias and the metal layers (five layers in this process) connecting the IMPATT diode to the antenna were again modeled using Sonnet as shown in Fig. 10.

After inserting Z_1, Z_2, and $C_{\rm tot}$, the simulation results reveal a degradation of the IMPATT real and imaginary parts by 25% and 5%, respectively.

C. Bias T

A dc bias (Fig. 11), which is well isolated from the RF, is created by utilizing a quarter-wavelength high-impedance microstrip line. One end is attached to the low-impedance point at the nonradiating edge of the patch antenna, minimizing the disturbance of the EM fields. The other end is terminated in a low-impedance pad, realized by a metal-to-metal capacitance structure of approximately 5 pF.

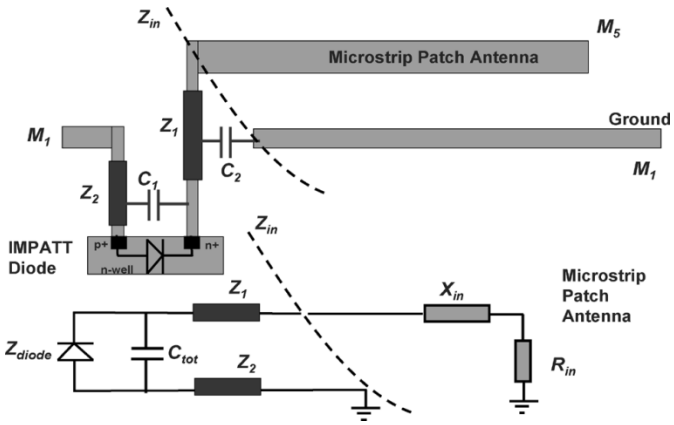

Fig. 10. Equivalent circuit of the monolithic IMPATT transmitter.

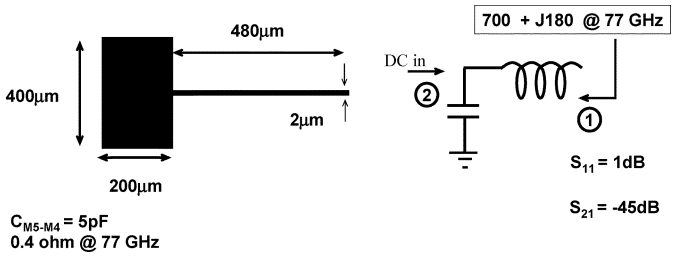

Fig. 11. Bias T and its equivalent circuit.

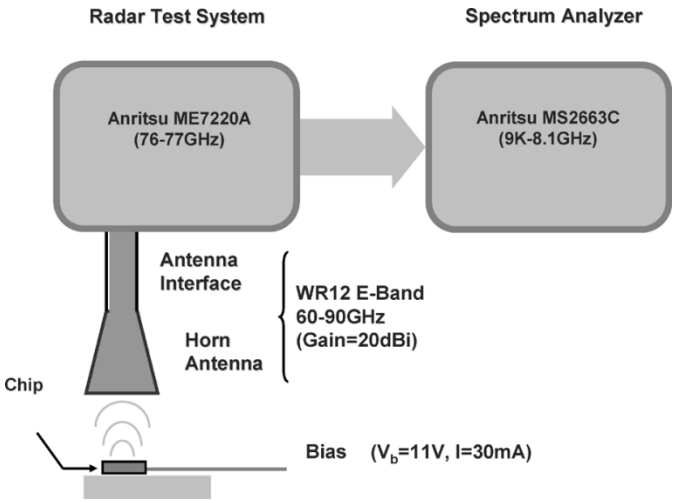

Fig. 12. Measurement setup, consisting of an Anritsu ME7220A RTS, WR12 E-band horn antenna, and MS2663C 9K-8.1-GHz spectrum analyzer.

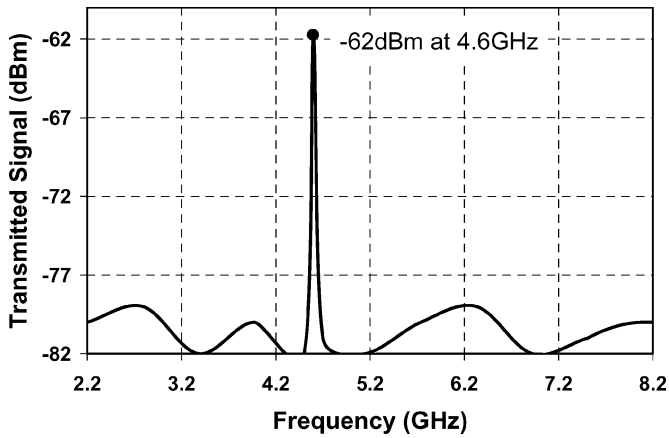

Fig. 13. Measurements of downconverted output signal.

TABLE I
CALCULATED AND MEASURED POWER

DC power delivered to the transmitter	330mW (25dBm)
DC losses, including: - feed line resistance - resistance of the diode inactive region	2dB
Power delivered to the IMPATT diode	200mW (23dBm)
Losses of the microstrip patch antenna, including: - dielectric losses - conduction losses - radiation losses	34dB
Losses of the measurement setup (from the horn antenna to the spectrum analyzer)	10dB
Measured transmitted power	-62dBm
Calculated power generated by the diode	-18dBm
Calculated diode efficiency	-41dB

III. MEASUREMENTS AND RESULTS

The test setup includes an Anritsu ME7220A radar test system (RTS), WR12 E-band horn antenna, and MS2663C 9K-8.1-GHz spectrum analyzer (Fig. 12). The frequency band of the transmitter is initially downconverted by the RTS from 76 to 77 GHz to an IF band of 4.7–5.7 GHz before the radiated signal is characterized. Initially, the supply is maintained at 0 V and slowly increased (to avoid any surges) up to the operating voltage of the diode. At the nominal breakdown voltage of $\sim$10 V, a current of 2 mA flows. As the supply voltage is gradually increased, the current drawn by the circuit also increases. When the on-chip transmitter is biased at 11 V, the corresponding quiescent current is 30 mA, and a signal is detected with an oscillation frequency of 76 GHz, as shown in Fig. 13. The measured oscillation frequency differs by only 1.3% from the predicted value of 77 GHz. Based on the measured radiated power and the system losses, the calculated diode efficiency is -41 dB. This low efficiency is largely a result of the high capacitive loading from the depletion region. In addition, other sources of loss, such as antenna surface roughness, are not included in our simulations. They can, in practice, further increase the total antenna losses, which, when taken into account, would result in a higher calculated IMPATT efficiency. In Table I, the calculated and measured radiated power levels are shown.

IV. Conclusion

A monolithic integrated IMPATT transmitter built in standard CMOS technology and operating in the millimeter-wave range has been investigated experimentally. Using a patch antenna driven by a lateral IMPATT diode, the 4-mm^2 transmitter delivers a radiated power of -62 dBm at 76 GHz. By using this particular configuration, area requirements and parasitic losses of the integrated transmitter are reduced. Because of the cost efficiency and the robustness of standard CMOS manufacturing, this type of monolithic integrated transmitter may be well suited for use in millimeter-wave systems for various applications ranging from communications to automobile anticollision radar systems.

Acknowledgment

The authors would like to thank National Semiconductor, Santa Clara, CA, for fabricating the monolithic transmitter, Sonnet Software, Syracuse, NY, for providing the simulation tool, and Anritsu, Morgan Hill, CA, for providing the RTS and the measurement setup.

References

[1] J. F. Luy and P. Russer, "SiGe SIMMWICs," in *IEEE Radio Frequency Integrated Circuits Symp.*, Denver, CO, Jun. 8–11, 1997, pp. 105–108.

[2] N. Camilleri and B. Bayraktaroglu, "Monolithic millimeter-wave IMPATT oscillator and active antenna," *IEEE Trans. Microw. Theory Tech.*, vol. 36, no. 12, pp. 1670–1676, Dec. 1988.

[3] B. Bayraktaroglu, "V-band monolithic IMPATT VCO," in *IEEE MTT-S Int. Microwave Symp. Dig.*, vol. 2, Baltimore, MD, May 25–27, 1988, pp. 687–690.

[4] E. M. Bieble, J. Muller, and H. Ostner, "Analysis of planar millimeter wave slot antennas using a spectral domain approach," in *IEEE MTT-S Int. Microwave Symp. Dig.*, vol. 1, Albuquerque, NM, Jun. 1–5, 1992, pp. 381–384.

[5] T. Al-Attar, M. Mulligan, and T. Lee, "Lateral IMPATT diodes in standard CMOS technology," in *Int. Electron Devices Meeting Dig.*, Washington, DC, Dec. 13–15, 2004, pp. 459–462.

[6] T. Al-Attar, A. Hassibi, and T. H. Lee, "A 77 GHz monolithic IMPATT transmitter in standard CMOS technology," in *IEEE MTT-S Int. Microwave Symp. Dig.*, Long Beach, CA, Jun. 2005. [CD ROM].

[7] S. M. Sze, *Physics of Semiconductor Devices*, 2nd ed. New York: Wiley, 1981, pp. 566–591.

[8] J. F. Luy, K. M. Strohm, J. Buechler, and P. Russer, "Silicon monolithic millimeter-wave integrated circuits," *Proc. Inst. Elect. Eng., Microw. Antennas Propag.*, vol. 139, no. 3, pp. 209–216, Jun. 1992.

[9] W. T. Read, Jr., "A proposed high-frequency negative-resistance diode," *Bell Syst. Tech. J.*, vol. 37, no. 2, pp. 401–446, Mar. 1958.

[10] P. J. Stabile and B. Lalevic, "Lateral IMPATT diodes," *IEEE Electron Device Lett.*, vol. 10, no. 6, pp. 249–251, Jun. 1989.

Talal Al-Attar was born in Kuwait, in 1970. He received the B.S. and M.S. degrees from Kuwait University, Kuwait, in 1995 and 1997, respectively, and the Ph.D. degree from Stanford University, Stanford, CA. His doctoral research concerned IMPATT transmitters in CMOS technology.

His research interests include IMPATT modeling at the millimeter-wave range, on-chip integration of microstrip patch antennas, and millimeter-wave monolithic circuits for anticollision radar systems.

Thomas H. Lee (S'87–M'88) received the S.B., S.M., and Sc.D. degrees in electrical engineering from the Massachusetts Institute of Technology (MIT), Cambridge, in 1983, 1985, and 1990, respectively.

In 1990, he joined Analog Devices, where he was primarily engaged in the design of high-speed clock recovery devices. In 1992, he joined Rambus Inc., Mountain View, CA, where he developed high-speed analog circuitry for 500-MB/s CMOS dynamic random access memories (DRAMs). He has also contributed to the development of phase-locked loops (PLLs) in the StrongARM, Alpha, and AMD K6/K7/K8 microprocessors. Since 1994, he has been a Professor of electrical engineering with Stanford University, Stanford, CA, where his research focus has been on gigahertz-speed wireline and wireless integrated circuits built in conventional silicon technologies, particularly CMOS. He cofounded Matrix Semiconductor, Santa Clara, CA. He authored *The Design of CMOS Radio-Frequency Integrated Circuits* (now in its second edition) (Cambridge, U.K.: Cambridge Univ. Press, 1998) and *Planar Microwave Engineering* (Cambridge, U.K.: Cambridge Univ. Press, 2004). He coauthored four additional books on RF circuit design. He holds 35 U.S. patents.

Dr. Lee is a Distinguished Lecturer of both the IEEE Solid-State Circuits Society and the IEEE Microwave Theory and Techniques Society (IEEE MTT-S). He has twice been the recipient of the Best Paper Award presented at the International Solid State Cicuits Conference (ISSCC). He coauthored a Best Student Paper at ISSCC. He was the recipient of the Best Paper prize at the Custom Integrated Circuits Conference (CICC) and was a Packard Foundation Fellowship recipient.